

SUPPORTING INFORMATION

Novel molecular insights into the critical role of sulfatide in myelin maintenance/function

Juan Pablo Palavicini^{1#}, Chunyan Wang^{1#}, Linyuan Chen¹, Sareen Ahmar¹, Juan Diego Higuera¹,
Jeffrey L. Dupree²⁻³, and Xianlin Han^{1,*}

¹Center for Metabolic Origins of Disease
Sanford Burnham Prebys Medical Discovery Institute
Orlando, Florida 32827

²Department of Anatomy and Neurobiology
Virginia Commonwealth University
Richmond, Virginia 23298

and
³Research Division
McGuire Veterans Affairs Medical Center
Richmond, VA 23249

Materials and methods

Internal standards were in a pre-mixed solution for global lipid analysis and included *d*18:1-N16:0 sulfatide (3.08 nmol/mg protein), *d*18:1-N15:0 CBS (8 nmol/mg protein), *d*18:1-N12:0 SM (2.73 nmol/mg protein), di16:1 PE (23.58 nmol/mg protein), di14:1 PC (26.25 nmol/mg protein), and di14:0 PS (19.91 nmol/mg protein) for brain samples. The amount of internal standards used for spinal cord samples was 1.5 times of those added to the brain samples. Internal standards for quantitation of individual molecular species of lipid classes were added to each brain tissue sample based on protein concentration prior to lipid extraction. Thus, the lipid content could be normalized to the protein content and quantified directly. These internal standards were selected because they represent <<1% of endogenous cellular lipid molecular species present as demonstrated by electrospray ionization mass spectrometry (ESI-MS) lipid analysis without addition of these internal standards. Each treated solution was finally reconstituted with a volume of 400 μ l/mg of tissue protein in 1:1 chloroform/methanol. All lipid solutions were finally flushed with nitrogen, capped, and stored at -20 °C for ESI-MS (typically analyzed within 1 week).

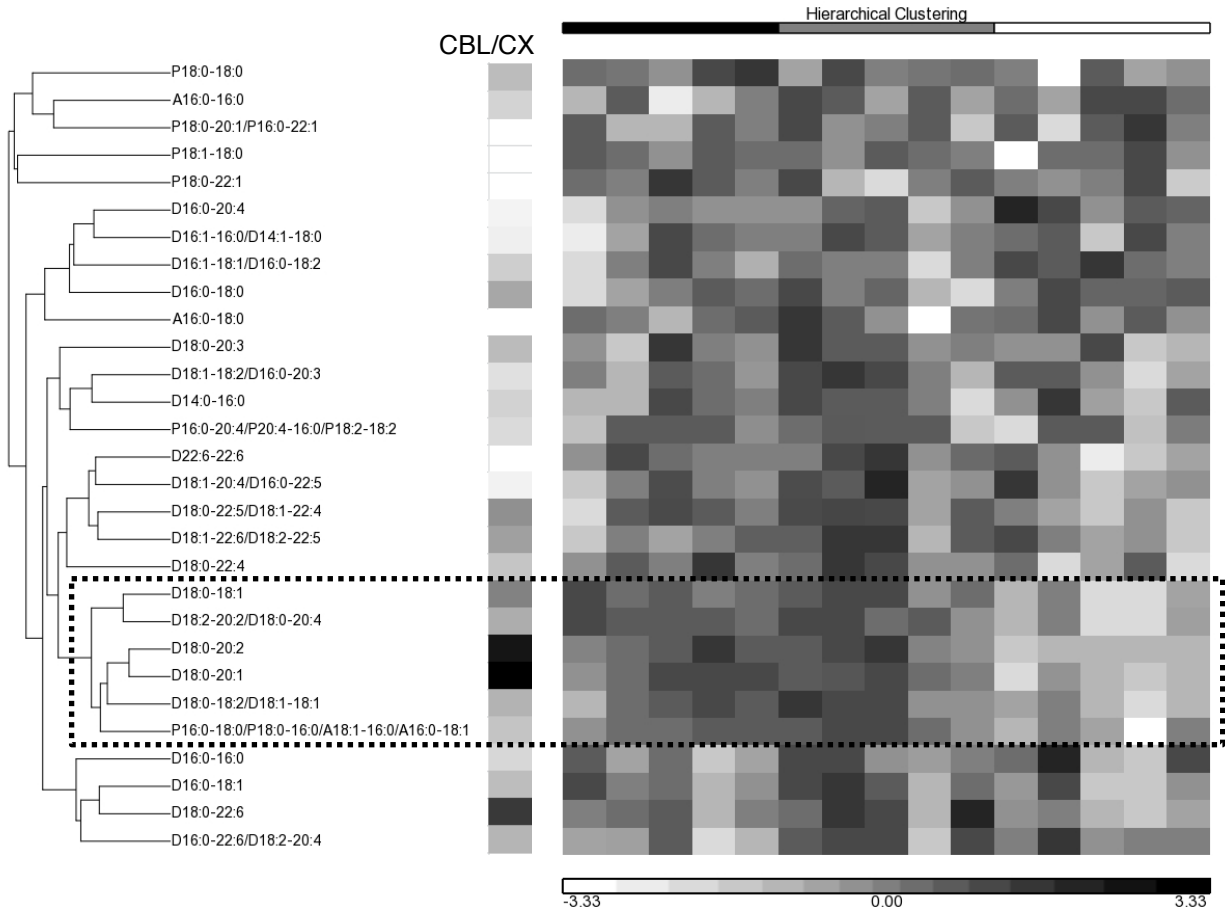


Figure S2. Hierarchical clustering for brain PC molecular species. The masses of each PC molecular species (nmol/mg) from 10 month old mouse cerebella were log-10 transformed for hierarchical clustering analysis using Euclidean dissimilarity and average linkage with Partek Genomics Suite software. The dendrogram shows how the 29 different PE molecular species (rows) were clustered together after grouping them into the 3 different genotypes (CST^{+/+}, +/-, -/- from left to right). The CBL/CX column depicts a heatmap of the [cerebellum]/[cortex] ratios. White represents the lowest CBL/CX ratio, while black represents the highest. The 15 column wide heatmap depicts the abundance of each molecular species on each individual animal analyzed (5 animals per genotype for this particular time point). Black represents the highest abundance and white the lowest. Note that the 6 molecular species that differed the most between the CST^{+/+} and CST^{-/-} (highlighted by a dotted rectangle) tend to be “myelin enriched” species (high CBL/CX ratios).

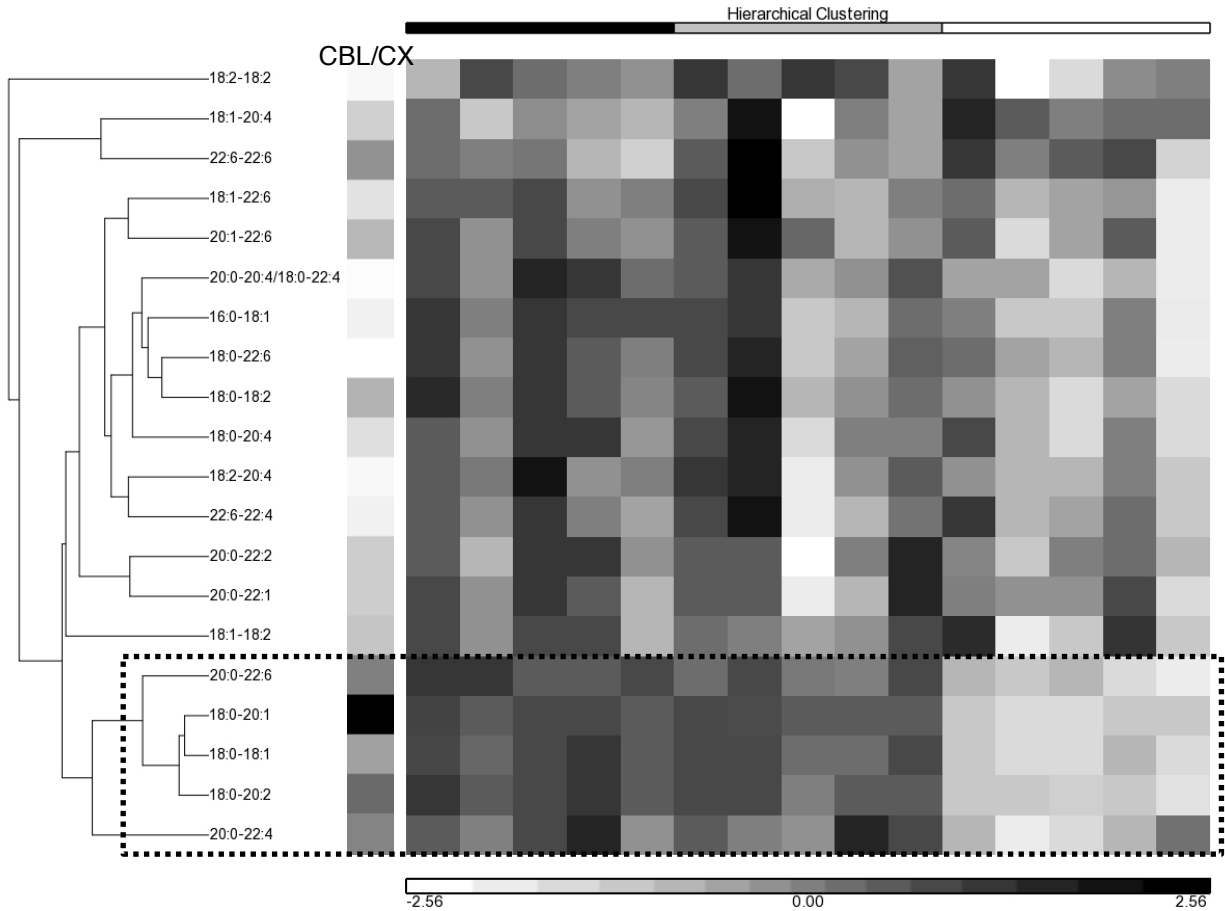


Figure S3. Hierarchical clustering for brain PS molecular species. The masses of each PC molecular species (nmol/mg) from 10 month old mouse cerebella were log-10 transformed for hierarchical clustering analysis using Euclidean dissimilarity and average linkage with Partek Genomics Suite software. The dendrogram shows how the 20 different PE molecular species (rows) were clustered together after grouping them into the 3 different genotypes (CST^{+/+}, CST^{+/-}, CST^{-/-} from left to right). The CBL/CX column depicts a heatmap of the [cerebellum]/[cortex] ratios. White represents the lowest CBL/CX ratio, while black represents the highest. The 15 column wide heatmap depicts the abundance of each molecular species on each individual animal analyzed (5 animals per genotype for this particular time point). Black represents the highest abundance and white the lowest. Note that the 5 molecular species that differed the most between the CST^{+/+} and CST^{-/-} (highlighted by a dotted rectangle) tend to be “myelin enriched” species (high CBL/CX ratios).

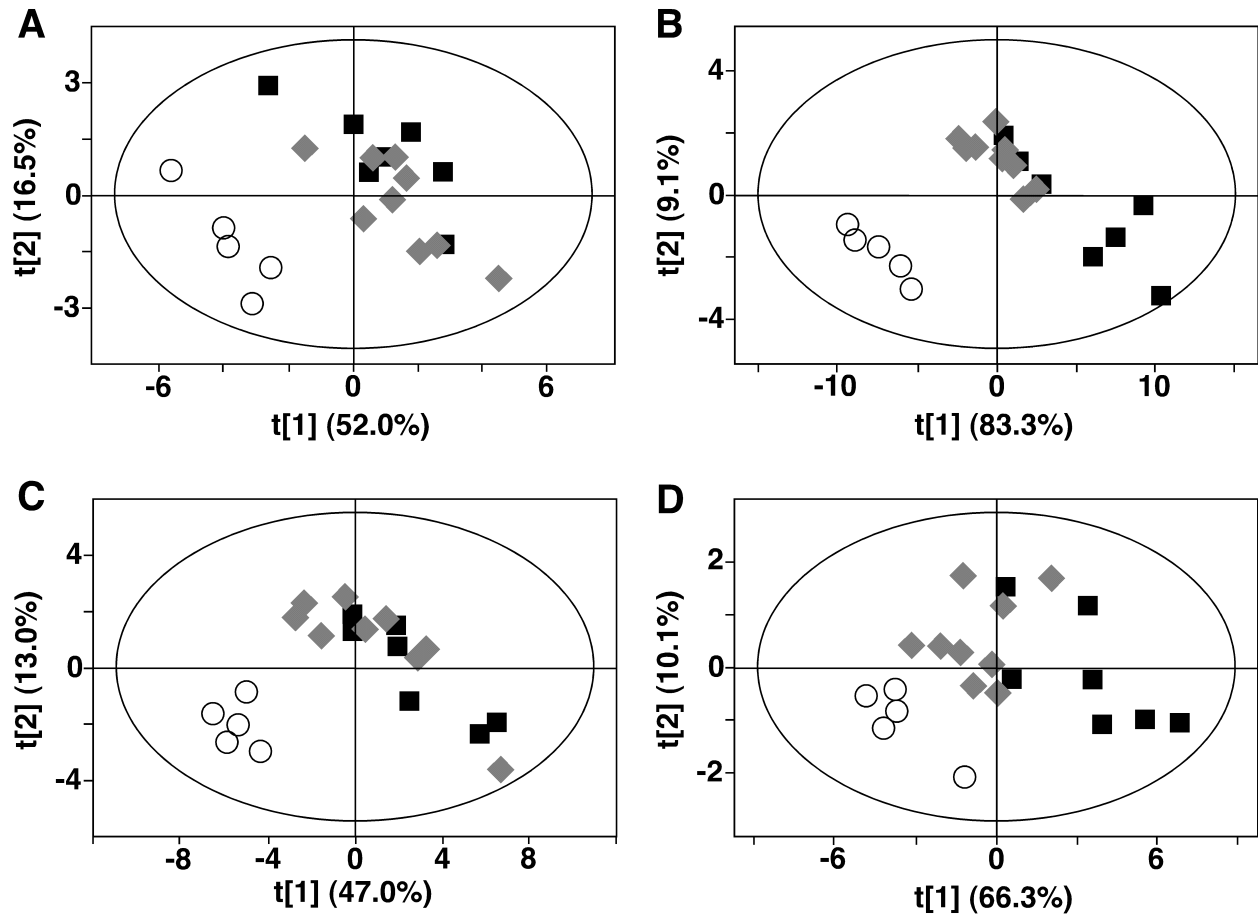


Figure S4. CST disruption leads to a differential abundance of specific phospholipid species. Partial least square-discriminate analysis (PLS-DA) score scatter plots and 95% Hotelling's T^2 ellipse from the global lipidomics profiles of specific lipid classes known to be abundant in the myelin including SM (a), PE (b), PC (c), and PS (d). Masses were transformed to the log-10 scale before running the analysis. $CST^{+/+}$ (black squares), $CST^{+/-}$ (gray diamonds), $CST^{-/-}$ (open circles).

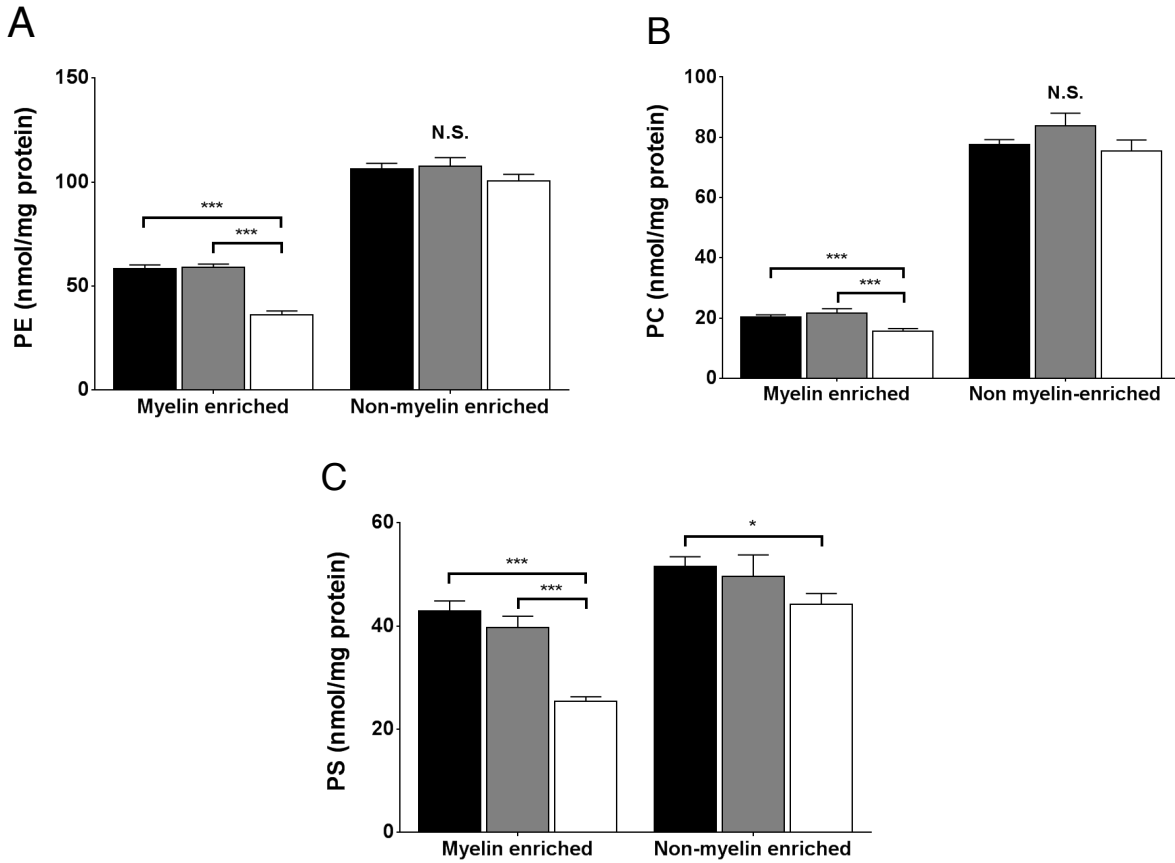


Figure S5. CST disruption exclusively alters myelin phospholipid homeostasis. Lipidomics analyses were performed on mouse cerebella from 10-months old CST+/+ (black bars), +/- (gray bars) and -/- (white bars) male mice (n = 5/genotype for this particular time point) by MDMS-SL as described in the section of “Materials and Methods”. Molecular species of the major phospholipid classes found in myelin were grouped as “myelin enriched” (CBL/CX ratio >2) or “non-myelin enriched” (CBL/CX ratio <2). The sum of the masses of all the “myelin enriched” and the “non-myelin enriched” molecular species for PE (A), PC (B), and PS (C) are plotted. The data represent means \pm SE from 5 separate animals. * $p < 0.05$ and *** $p < 0.001$ as indicated.

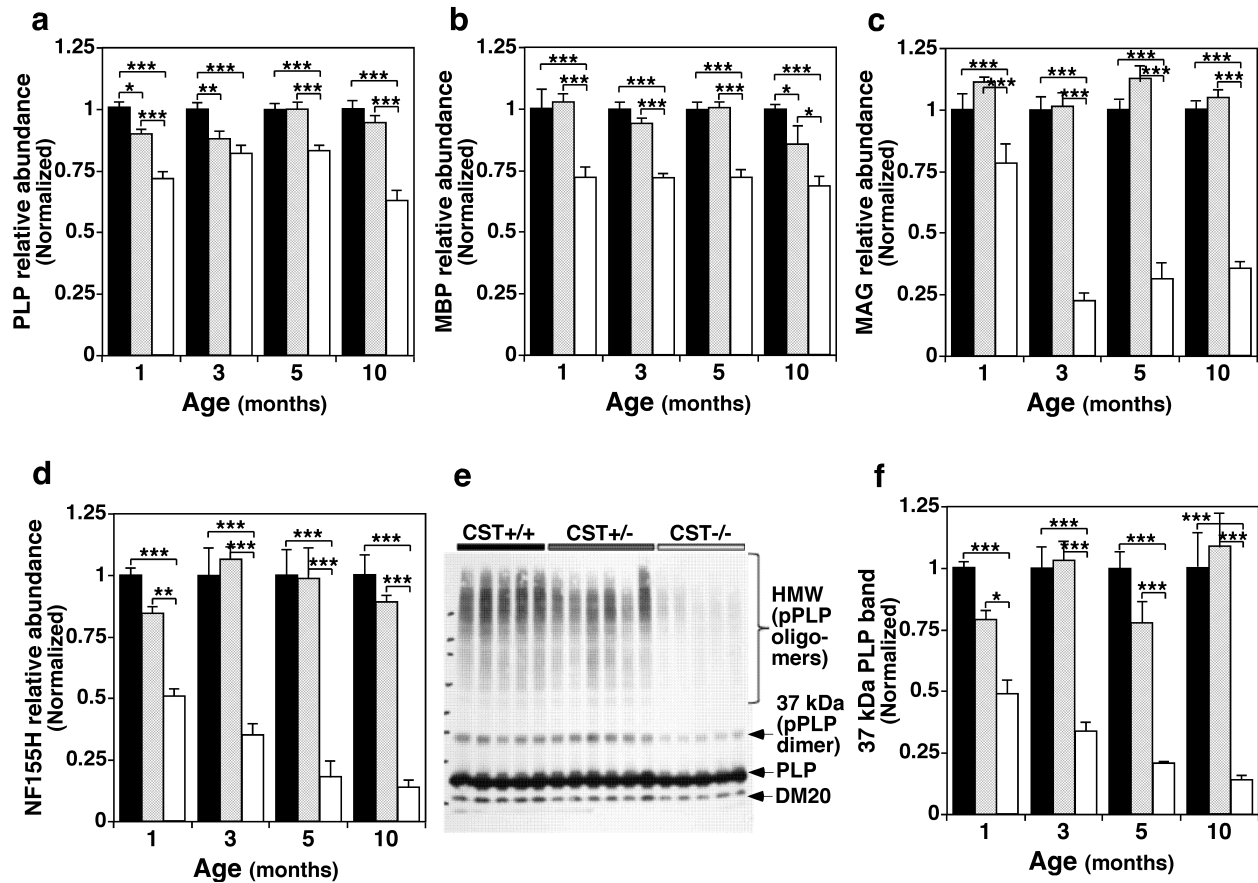


Figure S6. Longitudinal effects of CST disruption on major CNS myelin proteins. Mouse cerebella from 1-, 3-, 5-, and 10-months old CST+/+ (black bars), +/- (gray bars), and -/- (white bars) male mice were homogenized. Western blots from cerebellar NP40 supernatants using antibodies against PLP (a), MBP (b), MAG (c), and NF155 (d) were quantified using *ImageJ* software and normalized to a loading control (GAPDH). (e) Representative highly exposed PLP Western blot indicating the high molecular weight putative PLP oligomers and the 37 kDa putative PLP dimer. (f) Relative intensities of the 37 kDa putative PLP dimer were also quantified. The data represent means \pm SE from at least 4 separate animals. * $p < 0.05$, ** $p < 0.01$, and *** $p < 0.001$ as indicated.